A Locking–Free Meshless Local Petrov-Galerkin (MLPG) Formulation for Thick & Thin Plates

Q. Li[1], J.Sorić[2], T. Jarak[2], S. N. Atluri[1]

Summary

In this paper, a locking-free meshless local Petrov-Galerkin (MLPG) formulation is developed for both thick and thin plate. Shear locking is eliminated by changing two dependent variables in the governing equations. The concept of three-dimensional solid plate is used in the current formulation. Numerical examples at both thin plate limit and thick plate limit are analyzed.

Introduction

Meshless local Petrov-Galerkin (MLPG) method is a truly meshless method, which requires no element or background cell in either interpolation or integration [1]. It was applied to the three-dimensional plate analysis in another paper in this conference [2], where promising results for thick plate were obtained. However, the drawback of shear locking appears in the case of thin plates of thickness to span ratio less than 1/20. In this paper, a locking-free formulation is developed and extends the analysis to both thick and thin plates.

The concept of a locking-free weak formulation was introduced by Atluri in 1992 [3]. By using this concept, the dependent variables of upper-lower nodal displacements in the thick plate formulation [2] are changed to mid-plane displacements and shear strain components in order to remove field inconsistency. The corresponding locking-free local symmetric weak form is constructed over cylindrical shaped local sub-domains surrounding each upper-lower node set. Moving least square (MLS) approximation is adopted in the interpolation of field variables in the in-plane direction. In order to study the accuracy of the proposed method, numerical examples are carried out at both the thin plate limit and thick plate limit.

MLPG formulation for 3-D plate

The 3-D plate concept retains the kinematics of three-dimensional continuum in the flat plate structures. The strong form governing equations are the linear momentum balance equations of 3-D solid

[1] Center for Aerospace Research & Education, University of California, Irvine, Irvine, CA. 92612, USA

[2] Faculty of Mechanical Engineering and Naval Architecture, University of Zagreb, 10000 Zagreb, I. Lučića 5, Croatia

$$\sigma_{ij,j} + b_i = 0.$$ (1)

The plate is discretized by the sets of two nodes on the upper and lower surfaces respectively. Instead of writing the global weak form for the governing equations, the MLPG method constructs the weak-form over local sub-domains, which are taken as cylinders standing between upper, lower surface around each node set. (Figure 1)
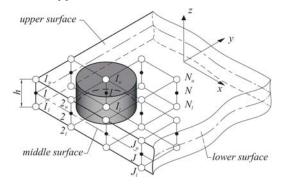

Figure 1 Nodal location and Local Sub-domain

The local weak form is

$$\int_{\Omega_s} \left(\sigma_{ij,j} + b_i\right) v_i d\Omega - \alpha \int_{\Gamma_{su}} (u_i - \bar{u}_i) v_i d\Gamma = 0,$$ (2)

where u_i is the trial function describing the displacement field, Ω_s is the local sub-domain, Γ_{su} is the part of the boundary of the local sub-domain with the prescribed displacement $\bar{u}_i$, and α denotes a penalty parameter. v_i is the linear test function

$$v_i = v_{0i} + x_3 v_{1i}.$$ (3)

Integration by parts and rearrange, a set of two governing equations for each local sub-domain can be derived.

$$\begin{cases} \int_{L_s} t_i d\Gamma + \int_{\Gamma_{su}} t_i d\Gamma + \int_{\Gamma_{st}} \bar{t}_i d\Gamma + \int_{\Omega_s} b_i d\Omega - \alpha \int_{\Gamma_{su}} (u_i - \bar{u}_i) d\Gamma = 0 \\ \int_{L_s} t_i x_3 d\Gamma + \int_{\Gamma_{su}} t_i x_3 d\Gamma + \int_{\Gamma_{st}} \bar{t}_i x_3 d\Gamma + \int_{\Omega_s} (b_i x_3 - \sigma_{i3}) d\Omega - \alpha \int_{\Gamma_{su}} (u_i - \bar{u}_i) x_3 d\Gamma = 0 \end{cases},$$ (4a, b)

where t_i represents the surface traction, $\bar{t}_i$ is its prescribed values, b_i is the body force. Please refer to Sorić et al [2] for detailed derivation.

Lock free Formulation

In order to reveal the locking phenomenon in the solid plate formulation, a local sub-domain with no crossing with boundary, no body force and no external force is examined. With these assumptions, equation 4a simply becomes the integration of surface traction over the side wall of a cylinder.

$$\int_{L_s} t_i d\Gamma = \int_{-\frac{h}{2}}^{\frac{h}{2}} \int_0^{2\pi} t_i R d\theta dx_3 = R \int_{-\frac{h}{2}}^{\frac{h}{2}} \int_0^{2\pi} n_j E_{ijkl} \frac{1}{2}\left(\frac{\partial u_k}{\partial x_l} + \frac{\partial u_l}{\partial x_k}\right) d\theta dx_3 , \quad (i,j,k=1,2,3), \quad (5)$$

where R is the radius of the cylindrical local sub-domain, h is the thickness of the plate, E_{ijkl} is tensor of elastic constants. If a linear interpolation is used through the thickness, plate deformation can be described by the displacement components as

$$\begin{cases} u_\alpha = u_{\alpha 0} + x_3 u_{\alpha 1} \\ u_3 = u_{30} + x_3 u_{31} \end{cases}, \qquad (\alpha = 1,2), \qquad (6)$$

where $u_{\alpha 0}$ and u_{30} are the mid-surface displacement, while $u_{\alpha 1}$ and u_{31} describe the rotations. Substitute (6) into (5) and integrate through the thickness, we have

$$\int_{L_s} t_i d\Gamma = Rh \int_0^{2\pi} n_j \left[E_{ij\alpha\beta} \frac{1}{2}\left(\frac{\partial u_{\alpha 0}}{\partial x_\beta} + \frac{\partial u_{\beta 0}}{\partial x_\alpha}\right) + E_{ij3\alpha}\left(\frac{\partial u_{30}}{\partial x_\alpha} + u_{\alpha 1}\right) + E_{ij33} u_{31} \right] d\theta = 0 ,$$
$$(\alpha, \beta = 1,2). \qquad (7)$$

It is obvious that the term $\left(\dfrac{\partial u_{30}}{\partial x_\alpha} + u_{\alpha 1}\right)$ produces spurious constraints at the thin plate limit, which give rise to overly stiff solution. In order to remove the above locking phenomenon, we assume

$$\gamma_\alpha = \frac{\partial u_{30}}{\partial x_\alpha} + u_{\alpha 1} . \qquad (8)$$

Substitute (8) into (6), we have

$$\begin{cases} u_\alpha = u_{\alpha 0} + x_3 \left(\gamma_\alpha - \dfrac{\partial u_{30}}{\partial x_\alpha} \right). \\[2mm] u_3 = u_{30} + x_3 u_{31} \end{cases} \tag{9}$$

Hence, the field variables $u_{\alpha 0}$, u_{30}, $u_{\alpha 1}$, u_{31} are changed to $u_{\alpha 0}$, u_{30}, γ_α, u_{31} and the field inconsistency is removed from the formulation. By applying the moving least square approximation, the displacement is discretized to

$$\begin{Bmatrix} u_1 \\ u_2 \\ u_3 \end{Bmatrix} = \sum_{i=1}^{n} \begin{bmatrix} \phi_i & 0 & -\phi_{i,1} x_3 & \phi_i x_3 & 0 & 0 \\ 0 & \phi_i & -\phi_{i,2} x_3 & 0 & \phi_i x_3 & 0 \\ 0 & 0 & \phi_i & 0 & 0 & \phi_i x_3 \end{bmatrix} \begin{Bmatrix} \hat{u}_{i10} \\ \hat{u}_{i20} \\ \hat{u}_{i30} \\ \hat{\gamma}_{i1} \\ \hat{\gamma}_{i2} \\ \hat{u}_{i31} \end{Bmatrix} = \sum_{i=1}^{n} \mathbf{\Phi}_i \hat{\mathbf{u}}_i , \tag{10}$$

where $\phi_i(x, y)$ is the shape function of the MLS approximation for the ith node, derived by employing the quadratic polynomial basis and 5th order spline of the weight function. $\hat{u}_{i\alpha 0}$, $\hat{u}_{i30}$, $\hat{\gamma}_{i\alpha}$, $\hat{u}_{i31}$ are the fictitious nodal values, and n is the total number of node sets in the domain of influence. Stresses can be calculated by taking the derivative of (10) and multiplying the constitutive matrix. Surface tractions can then be calculated by multiplying the normal with the stresses. Therefore, the discretized governing equations for each local sub-domain have the final form of

$$\begin{cases} \displaystyle\sum_{i=1}^{n} \left[\int_{L_s} \mathbf{NDB}_i d\Gamma + \int_{\Gamma_{su}} \mathbf{NDB}_i d\Gamma - \alpha \int_{\Gamma_{su}} \mathbf{\Phi}_i d\Gamma \right] \hat{\mathbf{u}}_i = -\int_{\Gamma_{st}} \bar{\mathbf{t}} d\Gamma - \int_{\Omega_s} \mathbf{b} d\Omega - \alpha \int_{\Gamma_{su}} \bar{\mathbf{u}} d\Gamma \\[4mm] \displaystyle\sum_{i=1}^{n} \left[\int_{L_s} \mathbf{NDB}_i x_3 d\Gamma + \int_{\Gamma_{su}} \mathbf{NDB}_i x_3 d\Gamma - \int_{\Omega_s} \mathbf{D'B'}_i d\Omega - \alpha \int_{\Gamma_{su}} \mathbf{\Phi}_i x_3 d\Gamma \right] \hat{\mathbf{u}}_i = -\int_{\Gamma_{st}} \bar{\mathbf{t}} x_3 d\Gamma - \int_{\Omega_s} \mathbf{b} x_3 d\Omega - \alpha \int_{\Gamma_{su}} \bar{\mathbf{u}} x_3 d\Gamma \end{cases} , \tag{11}$$

where $\mathbf{B}_i$ is the strain-displacement matrix obtained by taking the derivatives of the shape functions, $\mathbf{D}$ is the three-dimensional constitutive matrix, and $\mathbf{N}$ is the matrix describing the outward normal on the surface of local sub-domain. For each local sub-domain, six equations in the form of (11) are generated as well as the six fictitious unknowns. The actual upper-lower nodal displacements are obtained from the solved fictitious values using equation (10).

Numerical Example

Simply supported square plates under uniformly distributed load are analyzed. A uniform thickness value of 1.0 is used for all the cases, while the span of the plate varies. The schematic of the plates is list in Figure 2. Because of the symmetry of the problem, only a quarter of the plate is modeled. Uniform nodal distribution of 9 by 9 nodes is used on both the upper plate surface and the lower plate surface. Isotropic material property of $E = 1.092 \times 10^{6}$, $\nu = 0$ is used for all the cases.
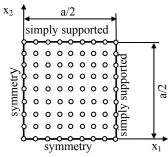

Figure 2 Simply supported plate under uniformly distributed load

At the thin plate limit, eight plates with span to thickness ratio between 20 and 1000 are analyzed. The maximum deflections normalized to the theoretical solution [4] are plotted in Figure 3. At the thick plate limit, six plates with thickness to span ratio between 5 and 10 are analyzed. Finite element analysis is carried out for the thick plate models due to the absence of theoretical solution. The maximum deflections from both FEM and MLPG are plotted in Figure 4. For both thick plate and thin plate, the locking-free MLPG formulation obtains accurate results.
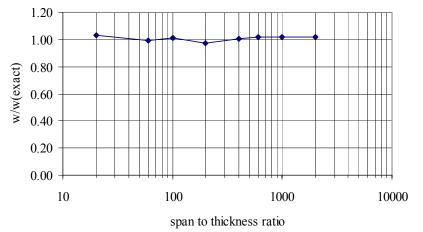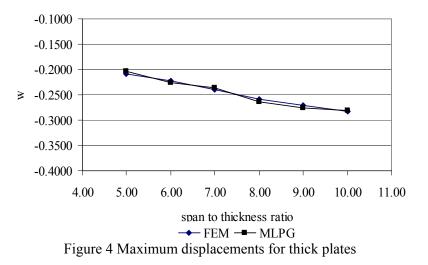

Figure 3 Maximum displacements for thin plates

Conclusion

A locking-free MLPG formulation for plate analysis employing a three-dimensional solid concept is presented in this paper. By changing the dependent variables, shear locking is completely eliminated. Numerical examples of simply-supported square plates under uniformly distributed load are carried out at both the thin plate limit and thick plate limit. Compared with analytical solution or finite element analysis, the current methodology shows accurate results for both thick and thin plates.

Figure 4 Maximum displacements for thick plates

Reference

1 Atluri, S. N. and Zhu, T. (1998): "A new meshless local Petrov-Galerkin (MLPG) approach in computational mechanics", *Comput. Mech.*, Vol. 22, pp. 117-127.

2 Sorić, J., Li, Q. and Jarak T., Atluri, S. N. (2004): "On application of meshless local Petrov-Galerkin (MLPG) method to analysis of shear deformable plates", *Submitted to ICCES'04*

3 Atluri, S. N. (1992): "Methods of computational mechanics", unpublished book

4 Timoshenko, S. (1940): "Theory of plate and shells", McGraw-Hill Book Company